

# Enhancement of Metabolic Oxidative Stress-Induced Cytotoxicity by the Thioredoxin Inhibitor 1-Methylpropyl 2-Imidazolyl Disulfide Is Mediated through the ASK1-SEK1-JNK1 Pathway

YONG J. LEE, JIN H. KIM, JUN CHEN, and JAE J. SONG

Department of Surgery, Pharmacology and Cancer Institute, School of Medicine (Y.J.L., J.H.K., J.J.S.), and Department of Neurology (J.C.), University of Pittsburgh, Pittsburgh, Pennsylvania

Received March 15, 2002; accepted September 3, 2002

This article is available online at <http://molpharm.aspetjournals.org>

## ABSTRACT

We observed previously that glucose deprivation induces cytotoxicity, increases the intracellular levels of hydroperoxide, and activates the stress-activated protein kinase (SEK) pathway. In this study, we hypothesized that 1-methylpropyl 2-imidazolyl disulfide (IV-2), a thioredoxin (TRX) inhibitor, augments glucose deprivation-induced cytotoxicity by promoting c-Jun N-terminal kinase (JNK) activation. Human prostatic carcinoma DU-145 cells were exposed to glucose-free medium containing various concentrations of IV-2 (10–50  $\mu$ M). Glucose deprivation alone or IV-2 alone induced minimal cytotoxicity within 7 h. However, the combination of glucose deprivation and IV-2 increased cell death in a dose-dependent manner. The cytotoxicity

was suppressed by treatment with an antioxidant, *N*-acetyl-L-cysteine or overexpressing TRX. The combined glucose deprivation and IV-2 treatment also promoted glucose deprivation-induced JNK1 activation by disrupting the interaction between TRX and apoptosis signal-regulating kinase 1 (ASK1). Overexpression of the JNK1 dominant-negative mutant inhibited the activation of the SEK pathway and protected cells from glucose deprivation and IV-2-induced cytotoxicity. Therefore, IV-2 enhances glucose deprivation-induced cytotoxicity by promoting glucose deprivation-induced activation of the ASK1-SEK1-JNK1 pathway.

We observed previously that glucose deprivation increases the intracellular levels of hydroperoxide and oxidized glutathione (Lee et al., 1998). Increases in steady-state levels of hydroperoxide during glucose deprivation seem to cause oxidative stress and cytotoxicity, which are inhibited by a thiol antioxidant such as *N*-acetyl-L-cysteine (NAC) (Blackburn et al., 1999). The fact that NAC inhibits glucose deprivation-induced increases in steady-state hydroperoxide levels, accumulation of oxidized glutathione, and cytotoxicity leads to the hypothesis that changes in the redox status of thiols are responsible for cell death during glucose deprivation. It is well known that all oxygen-metabolizing cells produce a rel-

atively constant low level of pro-oxidants (i.e., superoxide, hydrogen peroxide, etc.) as by-products of electron transport chain activity. The redox state is balanced by the cellular antioxidant capacity to maintain a viable nonequilibrium steady-state environment that is predominantly reducing. The major mechanism by which cells regulate redox processes is the reversible formation of disulfides through the oxidation of cysteine residues (Aslund and Beckwith, 1999).

One of the well-known redox regulatory systems involving disulfide formation is the thioredoxin/thioredoxin reductase system (Holmgren, 1985). Thioredoxin (TRX) is a 104 amino acid protein with a molecular mass of 12 kDa. It is a multifunctional and ubiquitous protein. It acts as a growth factor (Wakasugi et al., 1990), an antioxidant (Spector et al., 1988), a transcription factor regulator (Matthews et al., 1992), and an antiapoptotic molecule (Iwata et al., 1997). Recent

This research was supported by National Cancer Institute grant CA48000 and Competitive Medical Research Funds of The University of Pittsburgh Medical Center Health System.

**ABBREVIATIONS:** NAC, *N*-acetyl-L-cysteine; IV-2, 1-methylpropyl 2-imidazolyl disulfide; SEK, stress-activated protein kinase; TRX, thioredoxin; JNK, c-Jun N-terminal kinase; NAC, *N*-acetyl-L-cysteine; ASK1, apoptosis signal-regulating kinase 1; DMEM, Dulbecco's modified Eagle medium; PBS, phosphate-buffered saline; PAGE, polyacrylamide gel electrophoresis; PMSF, phenylmethylsulfonyl fluoride; Ad.TRX, adenoviral vector containing TRX; ROS, reactive oxygen species; m.o.i., multiplicity of infection; 8-OhdG, 8-hydroxyl-2'-deoxyguanosine; 2-dG, 2-deoxyguanosine; MEK, mitogen-activated protein kinase kinase; MAPK, mitogen-activated protein kinase; HPLC-EC, high-performance liquid chromatography with electrochemical detection; pfu, plaque-forming units; HA, hemagglutinin; GST, glutathione S-transferase; Ad.ASK1, HA-tagged ASK1; pcDNA3-FLAG-JNK1(APF), dominant-negative mutant c-Jun N-terminal kinase 1 cDNA; HA, hemagglutinin.

studies reveal that TRX is a binding partner of apoptosis signal-regulating kinase 1 (ASK1) (Saitoh et al., 1998). TRX associated with the N-terminal portion of ASK1 and the interaction between them is highly dependent on the redox state of TRX. The dissociation of TRX from ASK1 activates the ASK1-MEK-MAPK signal transduction pathway, thus promoting cell death via apoptosis (Ichijo et al., 1997). In this study, we hypothesized that inhibiting TRX function would augment glucose deprivation-induced cytotoxicity by promoting the ASK1-MEK-MAPK signal transduction pathway. Among a series of imidazolyl disulfide compounds that inhibit TRX activity through thioalkylation of critical cysteine residues (Kirkpatrick et al., 1998), we chose the most potent and selective TRX inhibitor, 1-methylpropyl 2-imidazolyl disulfide (IV-2). Our studies demonstrate that glucose deprivation-induced cytotoxicity and oxidative DNA damage are significantly enhanced by treatment with IV-2. This is probably caused by the promotion of a glucose deprivation-activated ASK1-SEK1-JNK1 pathway by treatment with IV-2.

## Materials and Methods

**Cell Culture and Survival Determination.** Human prostatic adenocarcinoma DU-145 cells were cultured in Dulbecco's modified Eagle's medium (DMEM) with 10% fetal bovine serum (Hyclone, Logan, UT) and 26 mM sodium bicarbonate. The Petri dishes containing cells were kept at 37°C in a humidified incubator with a mixture of 95% air and 5% CO<sub>2</sub>. Two days before the experiment, cells were plated into 60-mm Petri dishes. For survival determination, cells were treated with trypsin, formed into pellets, and resuspended in 0.2 ml of DMEM, 0.5 ml of 0.4% trypan blue solution, and 0.3 ml of phosphate-buffered saline solution (PBS). The samples were mixed thoroughly, incubated at room temperature for 15 min, and examined.

**Measurement of 8-OHdG Content.** The content of 8-hydroxyl-2'-deoxyguanosine (8-OHdG) in nuclear DNA was measured using high-performance liquid chromatography with electrochemical detection (HPLC-EC) as described previously (Lan et al., 2000). The stock standard solution containing 8-OHdG or 2-deoxyguanosine (2-dG) (Sigma, St. Louis, MO) was prepared at 1 mg/ml and stored at 4°C. This stock then underwent a 100-fold dilution (10 µg/ml) and was used directly as a standard. All other chemicals were the purest that was commercially available. The water used in all experiments was obtained from a Milli-Q water purification system (Millipore Corporation, Bedford, MA) and measured at 18.2 MΩ-cm.

The method for DNA extraction and subsequent digestion was the same as that described previously (Lan et al., 2000). This protocol avoided the use of phenol or any known oxidants that may induce background 8-OHdG. Briefly, cells were kept in a hypotonic buffer for the isolation of nuclei (Nagayama et al., 2000). The pellet containing the nuclei was then suspended at 1:5 (v/v) in the lysis buffer containing 1 M LiCl, 2 M urea, 40 mM sodium citrate, 5 mM EDTA, and 2% SDS. RNase A (final concentration, 0.1 mg/ml) and proteinase K (final concentration, 0.2 mg/ml) were added to each sample and incubated for 2 h at 50°C. The aqueous solution containing the nucleic acids was extracted with three changes of chloroform/isoamyl alcohol (24:1, v/v). The aqueous solution and chloroform/isoamyl alcohol were mixed for 15 min between changes and centrifuged for 20 min at 10,000g (Beckman J2-MC; Beckman Coulter, Inc., Fullerton, CA). The final aqueous extraction was removed, and a 1/15 volume of 3 M sodium acetate, pH 7.0, and 2 volumes of 95% cold ethanol were added. DNA was precipitated at -20°C overnight. The sample was centrifuged at 13,000g for 30 min to form a pellet. The DNA pellet was air-dried and resuspended in 100 µl of buffer containing 10 mM Tris, pH 7.4, and 1 mM EDTA. The DNA concentra-

tion was measured using a spectrophotometer (Beckman Coulter, Fullerton, CA).

DNA digestion was performed using nuclease P1 and alkaline phosphatase to circumvent possible contamination by trace metals in DNase I. A 10-µl aliquot of 0.5 M sodium acetate, pH 5.1, and 1.0 µl of 1 M magnesium chloride were added to the above DNA solution. The sample was then boiled at 100°C for 5 min and immediately cooled on ice for 5 min. A 4-µl aliquot of nuclease P1 (1 mg/ml) was added, and the sample was then incubated for 1 h at 37°C. After adjusting the pH to 7.8 by adding a 4-µl aliquot of 1 M Tris, pH 10.6, 1 µl of alkaline phosphatase (1 U/µl) was added. The sample was then incubated for 1 h at 37°C. Enzymes were precipitated by adding 2 µl of 5.8 M acetic acid, and then the sample was filtered through a 0.2-µm HPLC filter. A 20-µl sample containing 2 µg of DNA was then injected into the HPLC. Samples were further diluted to 1:100 in water for the analysis of 2-dG.

The isocratic analysis was conducted using a CoulArray system (model 5600) equipped with a dual piston pump (model 580) and a PEEK pulse damper (ESA, Inc., Chelmsford, MA). The analysis was performed using two coulometric array cell columns. The data were acquired and analyzed using the CoulArray software. The data were expressed as the amount of 8-OHdG in 10<sup>5</sup> 2-dG determined in the same sample (Lan et al., 2000). Using a syringe sample injector (model 9125; RHEODYNE, Cotati, CA), the samples were separated on a 3-µm 150 × 4.6-mm YMC basics C18 column (YMC, Wilmington, NC). The mobile phase contained 100 mM sodium acetate, pH 5.2, with phosphoric acid and methanol (95:5, v/v). The detector potentials were 200/290/380/520/730/800/870/940 mV (versus potential difference). The flow rate for the system was 1.0 ml/min.

**Glucose Deprivation and Drug Treatment.** Cells were rinsed three times (for 5 min each) with PBS solution, which took approximately 15 min. Cells were exposed to glucose-free DMEM with 10% dialyzed fetal bovine serum (Invitrogen, Carlsbad, CA). For drug treatment, cells were replaced with medium containing IV-2 (10–50 µM; a gift from Dr. D. L. Kirkpatrick, ProLX Pharmaceuticals, Pittsburgh, PA) and/or *N*-acetyl-L-cysteine (1–10 mM; Sigma).

**Morphological Evaluation.** Approximately 7 × 10<sup>5</sup> cells were plated into 60-mm Petri dishes overnight. Cells were exposed to glucose-free medium with or without IV-2 and then analyzed by phase-contrast microscopy.

**Transfection.** Cells were transfected with 0.5 to 2 µg of plasmids containing dominant-negative mutant c-Jun N-terminal kinase 1 (JNK1) cDNA [pcDNA3-FLAG-JNK1(APF); provided by R. Davis, University of Massachusetts Medical Center, Worcester, MA] by using Lipofectin reagent (Invitrogen). Cells were incubated for 48 h before the experiment.

**Adenoviral Vector Construction.** The adenovirus construct containing the transgene for human catalase was kindly provided by Dr. Beverly Davidson (Gene Transfer Vector Core, University of Iowa, Iowa City, IA). To construct a replication-incompetent adenoviral vector containing the cytomegalovirus promoter-driven thioredoxin gene (Ad.TRX), we used the *Cre-lox* recombination system (Hardy et al., 1997). In brief, a his-tagged 324-base pair TRX gene was isolated from pcDNA3.His-TRX (Hirota et al., 2000) by restriction digestion with *EcoRI* and cloned into the *EcoRI* site of the pAdlox shuttle vector. The complete shuttle vector was cotransfected into Cre8 cells with  $\psi$ 5 viral genomic DNA for homologous recombination. Plaques were harvested, analyzed, and purified.

**In Vivo Binding of ASK1 and TRX.** To examine the interaction between ASK1 and TRX, adenovirus of HA-tagged ASK1 (10 m.o.i.) and His-tagged TRX (20 m.o.i.) were coinfecting into DU-145 cells in 10-cm Petri dishes. For immunoprecipitation, cells were lysed in a lysis buffer containing 150 mM NaCl, 20 mM Tris-HCl, pH 7.5, 10 mM EDTA, 1% Triton X-100, 1% deoxycholate, 1 mM phenylmethylsulfonyl fluoride (PMSF), 80 µM aprotinin, and 2 mM leupeptin. Lysates were clarified by centrifugation at 15,000g for 15 min at 4°C. Proteins from the supernatant were immunoabsorbed with 2 µg of anti-penta His mouse IgG1 (QIAGEN, Valencia, CA) for 2 h. After

the addition of protein G/A agarose (Calbiochem, Darmstadt, Germany), the lysates were incubated for an additional 2 h. The beads were washed three times with the lysis buffer, separated by SDS-polyacrylamide gel electrophoresis (PAGE), and immunoblotted with rat anti-HA monoclonal antibody (clone 3F10; Roche Diagnostics, Mannheim, Germany) or mouse anti-penta His monoclonal antibody (QIAGEN). The proteins were detected with the enhanced chemiluminescence system (Amersham Biosciences Inc., Piscataway, NJ).

**In Vitro Kinase Assay.** The plasmid of GST-human JNK1 for bacterial fusion protein was constructed in pGEX-4T-1 by inserting *HindIII/XbaI* fragment followed by Klenow treatment from pcDNA3-JNK1. The expression of GST-JNK1 protein was confirmed by Western blotting and was purified by using glutathione Sepharose 4B (Amersham Biosciences). GST-SEK1 was purified from 293 cells transfected with the pEBG/SEK1 (kindly provided by J.M. Kyriakis, Massachusetts General Hospital, Charlestown, MA), and the purification step was performed as described previously (Yuasa et al., 1998). DU-145 cells were infected with 10 m.o.i. of Ad.HA-ASK1 for 24 h. After 24 h, cells were lysed in a buffer solution containing 20 mM Tris-HCl, pH 7.5, 150 mM NaCl, 5 mM EGTA, 10 mM NaF, 1% Triton X-100, 0.5% deoxycholate, 3 mM dithiothreitol, 1 mM sodium orthovanadate, 1 mM PMSF, and protein inhibitor cocktail solution (Sigma). Cell extracts were clarified by centrifugation, and the supernatants were immunoprecipitated with mouse anti-HA antibody (12CA5, Roche) and protein G/A agarose. The beads were washed twice with a solution containing 150 mM NaCl, 20 mM Tris-HCl, pH 7.5, 5 mM EGTA, 2 mM dithiothreitol, and 1 mM PMSF and washed once with the kinase buffer solution. To measure immune complex kinase activity, 0.2  $\mu$ g of GST-SEK1 was first incubated with the immune complexes for 10 min at 30°C in a final volume of 25  $\mu$ l of a solution containing 20 mM Tris-HCl, pH 7.5, 20 mM MgCl<sub>2</sub>, and 100  $\mu$ M ATP and subsequently with 1  $\mu$ g of GST-JNK1 for 10 min at 30°C. Thereafter, the activated complex was subjected to SDS-PAGE, and the phosphorylated JNK1 was detected with anti-ACTIVE JNK polyclonal antibody (Promega, Madison, WI). To determine the amount of ASK1 protein in the same sample, the upper part of the SDS-PAGE (>116 kDa) was cut out and immunoblotted with the mouse anti-HA antibody (Roche).

**Protein Extracts and PAGE.** Cells were lysed with 1 $\times$  Laemmli lysis buffer (2.4 M glycerol, 0.14 M Tris, pH 6.8, 0.21 M SDS, 0.3 mM bromophenol blue) and boiled for 10 min. Protein content was measured with the use of bicinchoninic acid protein assay reagent (Pierce Chemical, Rockford, IL). The samples were diluted with 1 $\times$  lysis buffer containing 1.28 M  $\beta$ -mercaptoethanol, and equal amount of protein was loaded on 8–13.5% SDS-PAGE. SDS-PAGE analysis was performed according to the method described by Laemmli (1970) using a Hoefer gel apparatus.

**Immunoblot Analysis.** Proteins were separated with the use of SDS-PAGE and electrophoretically transferred to a nitrocellulose membrane. The nitrocellulose membrane was blocked with 7% non-fat dry milk in PBS-Tween 20 (0.1%, v/v) at 4°C overnight. The membrane was incubated with anti-HA, anti-His, anti-JNK1 polyclonal (Santa Cruz Biochemicals, Santa Cruz, CA), or anti-ACTIVE JNK antibody (diluted according to the manufacturer's instructions) for 1 h. Horseradish peroxidase-conjugated anti-rabbit, anti-rat, or anti-mouse IgG was used as the secondary antibody. Immunoreactive protein was visualized by the enhanced chemiluminescence protocol (Amersham Biosciences).

## Results

**IV-2 Enhances Glucose Deprivation-Induced Cytotoxicity.** The effect of glucose deprivation on cell death in combination with IV-2, a thioredoxin inhibitor, was assessed in the human prostatic adenocarcinoma DU-145 cell line. Figure 1A shows that DU-145 cells starved for glucose exhibited a time-dependent reduction in cell survival. IV-2 alone

caused little or no cytotoxicity within 7 h. Figure 1A also shows that the glucose deprivation-induced cytotoxicity was markedly enhanced by adding IV-2 into the medium. Survival was dependent on the concentration of IV-2 added (10–50  $\mu$ M). For example, the survival of the cells decreased to 13% by 3 h of incubation in glucose-free medium with 50  $\mu$ M IV-2. These observations were consistent with morphological features (Fig. 1B). Cells treated with IV-2 in the absence of glucose underwent morphological alteration (rounding and blebbing formation) (Fig. 1B, d and e). Morphological changes were dependent on the dose of IV-2. More blebbing and rounding cells were observed at the higher concentrations of the drug. Figure 1C also shows that the combination of glucose deprivation and IV-2-induced cytotoxicity was inhibited by adding glucose into the glucose-free medium. DU-145 cells were treated with 50  $\mu$ M IV-2 in the presence of various concentrations of glucose (0.001–10 mM). Survival was dependent on the concentration of glucose added into the glucose-free medium. Little or no change in survival was gained by adding glucose up to a concentration of 0.01 mM, and then the survival of the cells increased linearly to 92% by adding glucose up to 1 mM. These results suggest that IV-2 promotes low glucose-induced cytotoxicity.

**Glucose Deprivation in Combination with IV-2 Enhances Oxidative DNA Damage.** We observed previously that glucose deprivation increases the intracellular level of reactive oxygen species (ROS) (Lee et al., 1998). It is well known that ROS causes oxidative DNA damage. To examine whether IV-2 enhances glucose deprivation-induced oxidative DNA damage, DU-145 cells were exposed to glucose-free medium in the presence of 50  $\mu$ M IV-2 for 3 h. After treatment, formation of the DNA base modification 8-OHdG was detected using HPLC-EC. Figure 2 shows a 2.5-fold increase in 8-OHdG content in the cells exposed to glucose-free medium in the presence of IV-2 compared with that in the absence of IV-2. Treatment with IV-2 itself caused an increase in 8-OHdG content. This is probably caused by the inhibition of TRX, which can scavenge ROS (Takemoto et al., 1998).

**Effect of the addition of N-Acetyl-L-Cysteine on Cells Starved for Glucose and Exposed to IV-2.** We reported previously that glucose deprivation induces metabolic oxidative stress (Lee et al., 1998). The metabolic oxidative stress-induced cytotoxicity is enhanced by IV-2, a thioredoxin inhibitor (Fig. 1). To confirm whether the effects of IV-2 on glucose deprivation are caused by an increase in oxidative stress, DU-145 cells were treated with an antioxidant, NAC, during incubation with glucose-free medium in the presence of IV-2. Figure 3A shows that IV-2 plus glucose deprivation-induced cytotoxicity was completely inhibited by treatment with NAC (1–10 mM). In addition, the morphological changes caused by glucose starvation and IV-2 were prevented by adding 1 mM NAC during treatment with 50  $\mu$ M IV-2 in the absence of glucose (Fig. 3B, d).

**Effect of Thioredoxin on the Cytotoxicity from the Combined Treatment of IV-2 and Glucose Deprivation.** To examine whether the overexpression of TRX could prevent cytotoxicity induced by IV-2 plus glucose deprivation, DU-145 cells were infected with Ad.TRX. Figure 4 shows a Western immunoblot demonstrating exogenous TRX protein expression as detected with a His-specific monoclonal antibody. Expression of TRX protein increased with increasing m.o.i.

(Fig. 4A) and increasing incubation period after infection (Fig. 4B). Expression of TRX was detected at an m.o.i. of 10 pfu/cell and greater. It was also detected after 16 h of incubation. To evaluate the effect of TRX overexpression on IV-

2-enhanced glucose-deprivation cytotoxicity, DU-145 cells were infected with Ad.TRX at various m.o.i. values and then exposed to medium containing 0.1 mM glucose and 50  $\mu$ M IV-2 for 4 h. We chose to use 0.1 mM glucose instead of

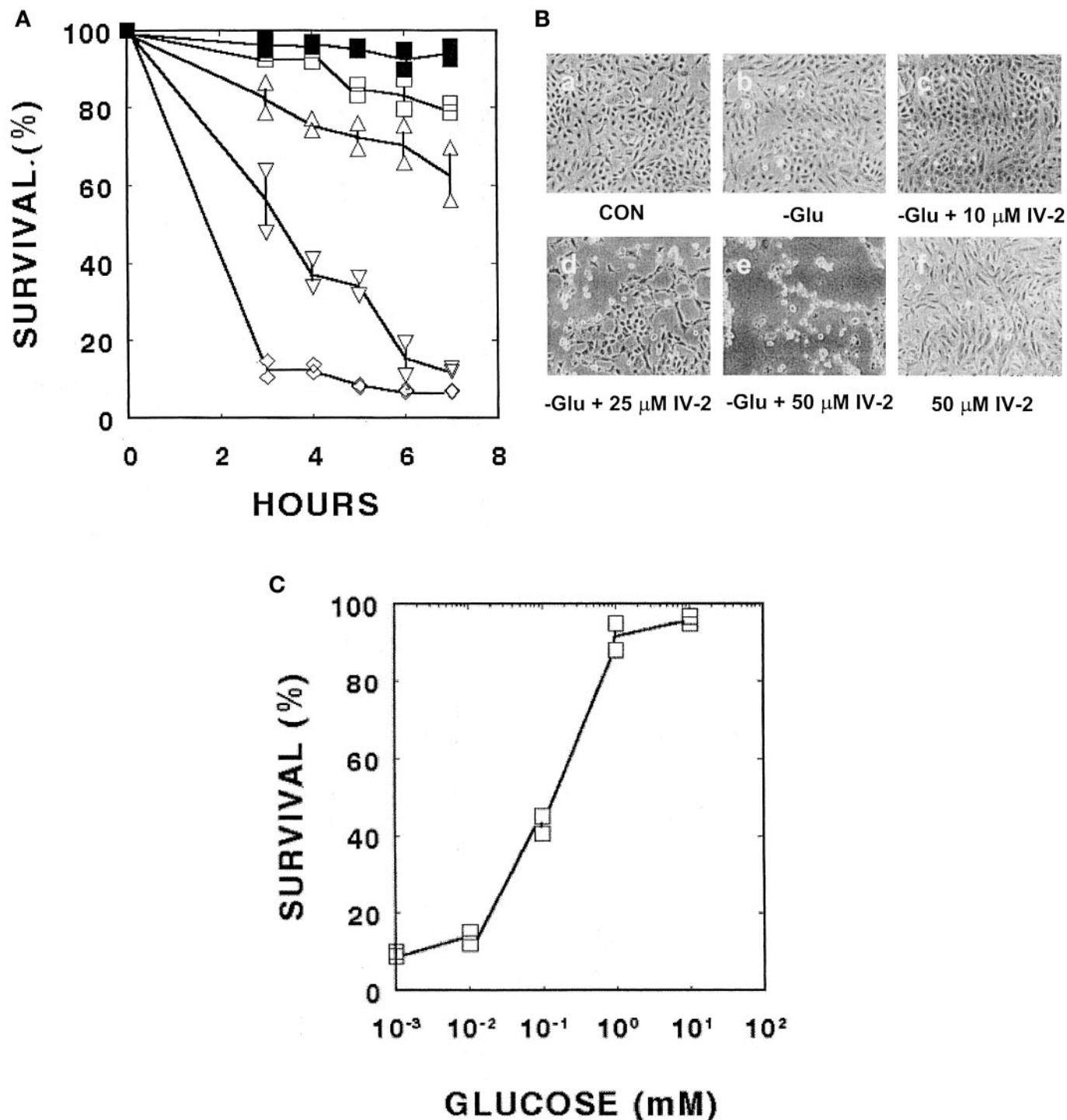


**Fig. 1.** Effect of IV-2 on glucose deprivation-induced cytotoxicity in DU-145 cells. A, cells were exposed to glucose-free medium in the presence of IV-2 (10–50  $\mu$ M) for various times, and cell survival was determined by use of the Trypan blue exclusion assay. (■), 50  $\mu$ M IV-2 alone; (□), glucose-free medium alone; (△), glucose-free medium plus 10  $\mu$ M IV-2; (▽), glucose-free medium plus 25  $\mu$ M IV-2; (◇), glucose-free medium plus 50  $\mu$ M IV-2. Data are a compilation of two separate experiments. B, cells were exposed to glucose-free medium alone (-Glu; b), 50  $\mu$ M IV-2 alone (50  $\mu$ M IV-2; f), or glucose-free medium in the combination with 10  $\mu$ M IV-2 (-Glu + 10  $\mu$ M IV-2; c), 25  $\mu$ M IV-2 (-Glu + 25  $\mu$ M IV-2; d), or 50  $\mu$ M IV-2 (-Glu + 50  $\mu$ M IV-2; e) for 4 h, and then morphological features were analyzed with phase-contrast microscopy. CON, untreated control cells (a). C, cells were treated with 50  $\mu$ M IV-2 in the presence of various concentrations (0.001–10 mM) of glucose for 4 h, and cell survival was determined by use of the Trypan blue exclusion assay. Data are a compilation of two separate experiments.

glucose-free medium because, as shown in Fig. 1C, transitional changes in the survival level can be easily detected in this range. Figure 4C shows that Ad.TRX infected cells became resistant to combined glucose deprivation and IV-2 treatment-induced cytotoxicity. Cells infected with Ad.TRX at an m.o.i. of 300 pfu/cell survived approximately 1.8-fold better than control adenoviral vector-infected cells.

**Activation of ASK1 by Glucose Deprivation and/or IV-2 Treatment.** Previous studies have shown that glucose deprivation induces an increase in intracellular hydroperoxide levels (Lee et al., 1998). In this study, we hypothesized that TRX recognizes metabolic oxidative stress and subsequently triggers ASK1 signal transduction pathway by disrupting the interaction between TRX and ASK1. To test our hypothesis, DU-145 cells were coinfecting with adenoviral vectors containing His-tagged TRX (Ad.TRX) and HA-tagged ASK1 (Ad.ASK1). Cells were exposed to glucose-free medium in the presence or absence of IV-2. Data from immunoprecipitation followed by immunoblot assay demonstrate that TRX dissociated from ASK1 during glucose deprivation (Fig. 5). The level of dissociation was enhanced by treatment with IV-2. These data suggest that IV-2 promotes the dissociation of TRX from ASK1.

**Combination of Glucose Deprivation and IV-2 Treatment Promotes JNK Activation.** We observed previously that glucose deprivation activates c-Jun N-terminal kinase 1 (JNK1 and overexpression of its dominant-negative mutant inhibits metabolic oxidative stress-induced cytotoxicity (Lee et al., 2000). We examined whether combined glucose deprivation and IV-2 treatment enhances JNK activation. JNK1 was activated within 5 min, and its activation was maintained for more than 2 h during glucose deprivation (Fig. 6A). Figure 6A also shows that glucose deprivation-induced JNK1 activation was promoted by treatment with IV-2. The level of

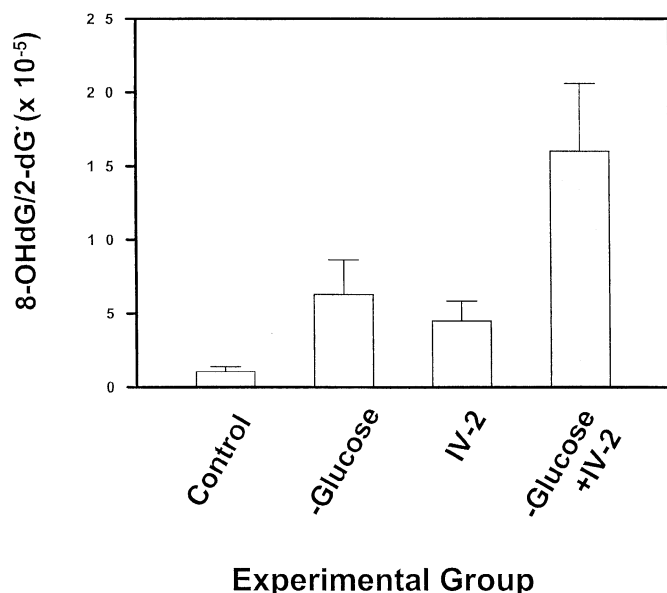


**Fig. 2.** Induction of 8-OHdG in nuclear DNA after glucose deprivation, IV-2 treatment, or glucose deprivation in combination with IV-2. DU-145 cells exposed to glucose free-medium alone (-Glucose), 50  $\mu$ M IV-2 alone (IV-2), or glucose-free medium in the presence of 50  $\mu$ M IV-2 (-Glucose + IV-2) for 3 h. Cells were harvested, and then 8-OHdG and 2-dG concentrations were measured using the HPLC-EC method. Data are mean  $\pm$  S.D. from triplicate samples.

activated JNK1 was dependent on the dose of IV-2. IV-2 itself also activates JNK1 (Fig. 6B). To examine whether combined glucose deprivation and IV-2 treatment promotes JNK1 activation by activating the ASK1-SEK1-JNK1 pathway, cells were infected with Ad.ASK1, and ASK1 kinase activity was measured by an immune complex-coupled kinase assay using glutathione *S*-transferase (GST)-SEK1 and GST-JNK1 as sequential substrates. Activated JNK1 was detected by anti-ACTIVE JNK1 antibody. Figure 7 shows the specificity of

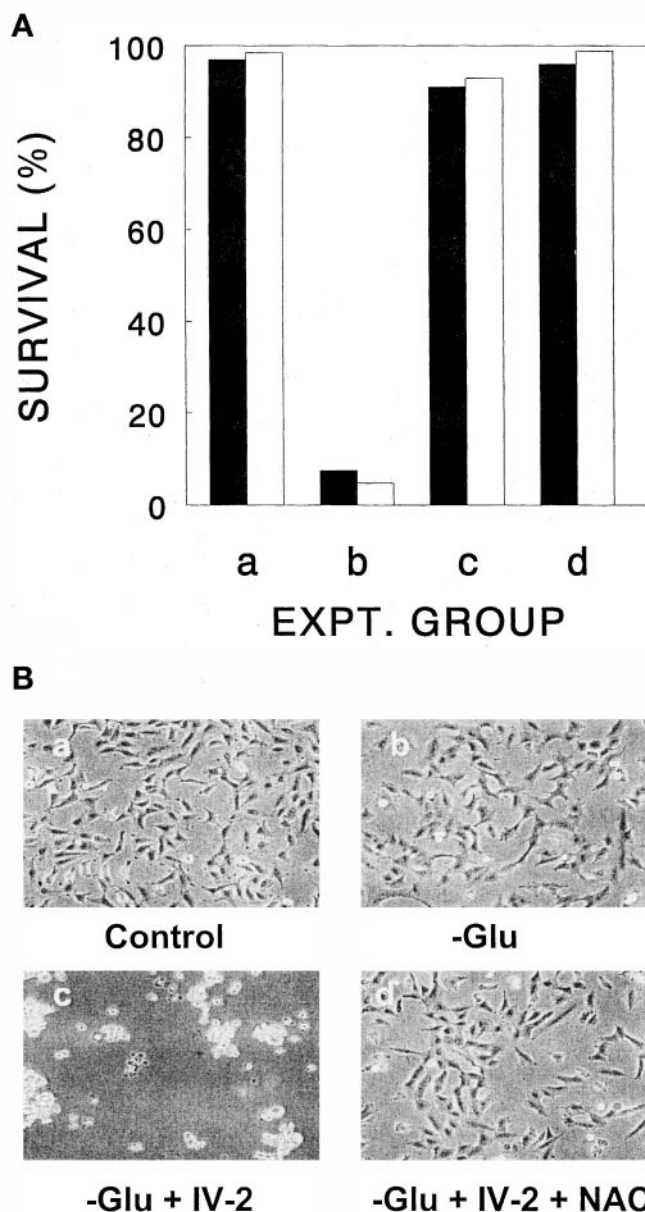


**Fig. 3.** Effect of NAC on the combination of glucose deprivation and IV-2 treatment-induced cytotoxicity. A, cells were incubated for 4 h with combined treatment of 50  $\mu$ M IV-2 and glucose deprivation in the presence of NAC, and then cell survival was determined by the Trypan blue exclusion assay. a, glucose-free medium alone; b, glucose-free medium plus 50  $\mu$ M IV-2; c, glucose-free medium plus 50  $\mu$ M IV-2 plus 1 mM NAC; d, glucose-free medium plus 50  $\mu$ M IV-2 plus 10 mM NAC. Data are a compilation of two separate experiments. B, morphology was also examined with phase-contrast microscopy. Control, untreated control cells (a); -Glu, cells were exposed to glucose-free medium alone for 4 h (b); -Glu + IV-2, glucose-free medium plus 50  $\mu$ M IV-2 (c); -Glu + IV-2 + NAC, glucose-free medium plus 50  $\mu$ M IV-2 plus 1 mM NAC (d).

ASK1-dependent phosphorylation of JNK1 in this assay. When cells were exposed to glucose-free medium, JNK1 was activated, and the activation of JNK1 was promoted by treatment with IV-2. These results illustrate that glucose deprivation activates the ASK1-SEK1-JNK1 signal transduction pathway, and the combined treatment of IV-2 and glucose deprivation facilitates this activation.

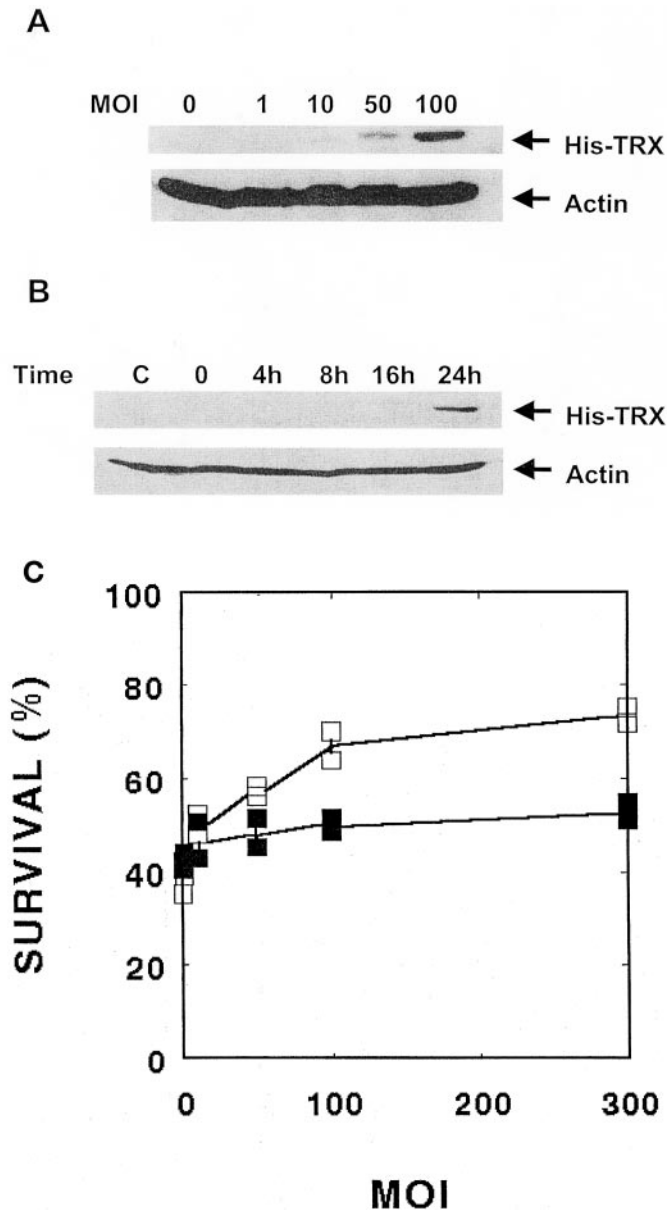


**Fig. 4.** Examination of TRX expression and its effect on glucose plus IV-2-induced cytotoxicity in adenovirus-infected cells. A, effect of m.o.i. on expression of TRX protein. Cells were infected with Ad.TRX at various m.o.i. values (0–100 pfu/cell) for 3 h and incubated for 24 h before harvested. B, time-dependent accumulation of TRX protein. Cells were infected with Ad.TRX at an m.o.i. of 100 pfu/cell for 3 h and incubated for various times (0–24 h) before harvesting. Lysates containing equal amounts of protein (20  $\mu$ g) were separated by the use of SDS-PAGE and immunoblotted by using anti-His monoclonal antibody-detected His-tagged TRX (His-TRX). Actin, actin was used to confirm that an equal amount of protein loaded in each lane. C, cells were infected with Ad.TRX (□) or control adenoviral vector (■) at various m.o.i. values (0–300 pfu/cell) for 3 h. After incubation for 24 h, cells were exposed to medium containing 0.1 mM glucose and 50  $\mu$ M IV-2 for 4 h before survival determination.

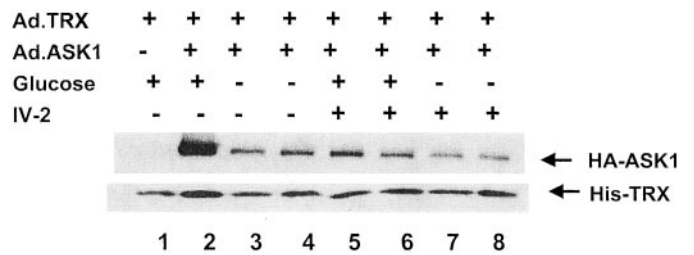


**Fig. 5.** Effect of IV-2 and/or glucose deprivation on the interaction of TRX with ASK1. Cells were coinfecting with adenoviral vectors containing His-tagged TRX (Ad.TRX) and HA-tagged ASK1 (Ad.ASK1) at an m.o.i. of 20 and 10 pfu/cell, respectively. After 24 h of incubation, cells were exposed to glucose-free medium for 10 min (lane 3) or 30 min (lane 4), or to 50  $\mu$ M IV-2 for 10 min (lane 5) or 30 min (lane 6), or to glucose-free medium plus IV-2 for 10 min (lane 7) or 30 min (lane 8). Proteins were immunoprecipitated with anti-His antibody and then immunoblotted with anti-HA antibody (top) or anti-His antibody (bottom).

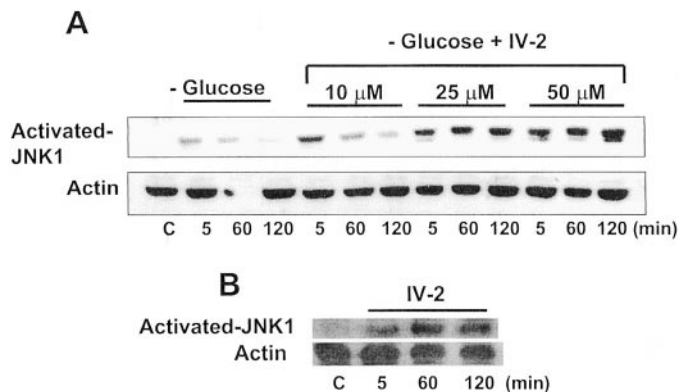


**Fig. 6.** Immunoblot detection of active JNK. A, cells were exposed to glucose-free medium (-Glucose) or glucose-free medium plus 10 to 50  $\mu$ M IV-2 (-Glucose + IV-2). B, cells were exposed to 50  $\mu$ M IV-2 alone (IV-2) for various times (5–120 min). After incubation, cells were harvested and Western blot analysis was performed as described in Fig. 4 with anti-ACTIVE JNK or anti-actin antibodies as the loading control.

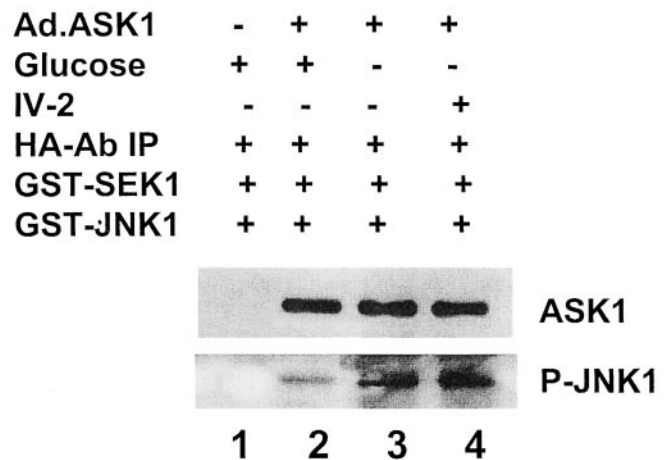


**Fig. 7.** Effect of IV-2 on glucose deprivation-activated ASK1-SEK1-JNK1 signal transduction. Cells were infected with Ad.ASK1 at an m.o.i. of 10 pfu/cell. After 24 h of incubation, cells were exposed to glucose-free medium for 1 h (lane 3) or glucose-free medium plus 50  $\mu$ M IV-2 for 1 h (lane 4). Lane 1, uninfected control cells; lane 2, Ad.ASK1 infection only. Proteins were immunoprecipitated with anti-HA antibody. The immune complex was incubated with GST-SEK1 and GST-JNK1 and then activated JNK1 (P-JNK1) was detected with anti-ACTIVE JNK.

**Effect of JNK1 Dominant-Negative Protein on the Combined Treatment of IV-2 and Glucose Deprivation-Induced JNK1 Activation and Cytotoxicity.** JNK1 activation has been implicated previously as the mechanism responsible for glucose deprivation-induced cytotoxicity; therefore, we examined the effect of JNK1 dominant-negative protein on the combined treatment of IV-2 and glucose deprivation. Cells were transiently transfected with control plasmid (pcDNA3-neo) or various concentrations (0.5 or 2  $\mu\text{g/ml}$ ) of dominant-negative JNK1 expression plasmid [pcDNA3-FLAG-JNK1(APF)]. JNK1 dominant-negative mutant protein was successfully expressed (Fig. 8A). Compared with wild-type JNK1 in either untransfected control cells or control plasmid-transfected cells, dominant-negative JNK1 was expressed approximately 12- to 19-fold in pcDNA3-FLAG-JNK1(APF) transfected cells, as determined by densitometric analysis. Control plasmid-transfected or dominant-negative JNK1 plasmid-transfected cells were treated with 50  $\mu\text{M}$  IV-2 in the absence of glucose. JNK1 was activated by glucose deprivation in combination with IV-2 (Fig. 8B, lane 2). Expression of JNK1 dominant-negative mutant protein suppressed this activation (Fig. 8B, lanes 4 and 6). We also tested the effect of expression of JNK1 dominant-negative mutant protein on the combined treatment of IV-2 and glucose deprivation-induced cytotoxicity. Expression of JNK1 dominant-negative mutant protein protected cells from this cytotoxicity (Fig. 8C). The degree of protection was dependent on the amounts of JNK1 dominant-negative mutant protein (Fig. 8A).

**Overexpression of Catalase Inhibits Glucose Deprivation Plus IV-2-Induced Dissociation of TRX from ASK1, JNK Activation, and Cytotoxicity.** To assess the involvement of ROS in glucose deprivation plus IV-2-induced dissociation of TRX from ASK1, JNK activation, and cytotoxicity, DU-145 cells were infected with adenoviral vectors containing catalase, an  $\text{H}_2\text{O}_2$  scavenger. Figure 9A shows that overexpression of catalase suppressed glucose deprivation plus IV-2-induced dissociation of TRX from ASK1 (Fig. 9A, lane 4 versus lane 3). Overexpression of catalase also inhibited glucose deprivation-induced JNK1 activation (Fig. 9B, lane 2 versus lane 5) as well as glucose deprivation plus IV-2-induced JNK1 activation (Fig. 9B, lane 3 versus lane 6). Overexpression of catalase prevented enhancement of glucose deprivation-induced cytotoxicity by IV-2 treatment (Fig. 9C).

## Discussion

Several conclusions can be drawn when considering the data presented. Glucose deprivation-induced cytotoxicity as well as JNK1 activation were augmented by treatment with IV-2, a TRX inhibitor. Overexpression of TRX or the dominant-negative mutant of JNK1 inhibited cytotoxicity and activation of JNK1. These results suggest that inhibiting TRX promotes metabolic oxidative stress and enhances cytotoxicity by increasing JNK1 activation.

In higher eukaryotes, ROSs are generated during respiration in mitochondria in the course of reduction of molecular oxygen. Our recent studies have demonstrated that glucose deprivation enhances the intracellular level of hydroperoxide (Lee et al., 1998). The most likely interpretation of our observations is that a decrease in the rate of elimination of ROS

via glutathione peroxidase/glutathione reductase, rather than an increased rate of mitochondrial oxidant production, is responsible for the increase in the level of hydroperoxide. The ROS produced in the mitochondria may not be eliminated sufficiently fast if NADPH is not produced quickly enough via the pentose phosphate pathway. Glucose deprivation also results in an increase in steady-state levels of

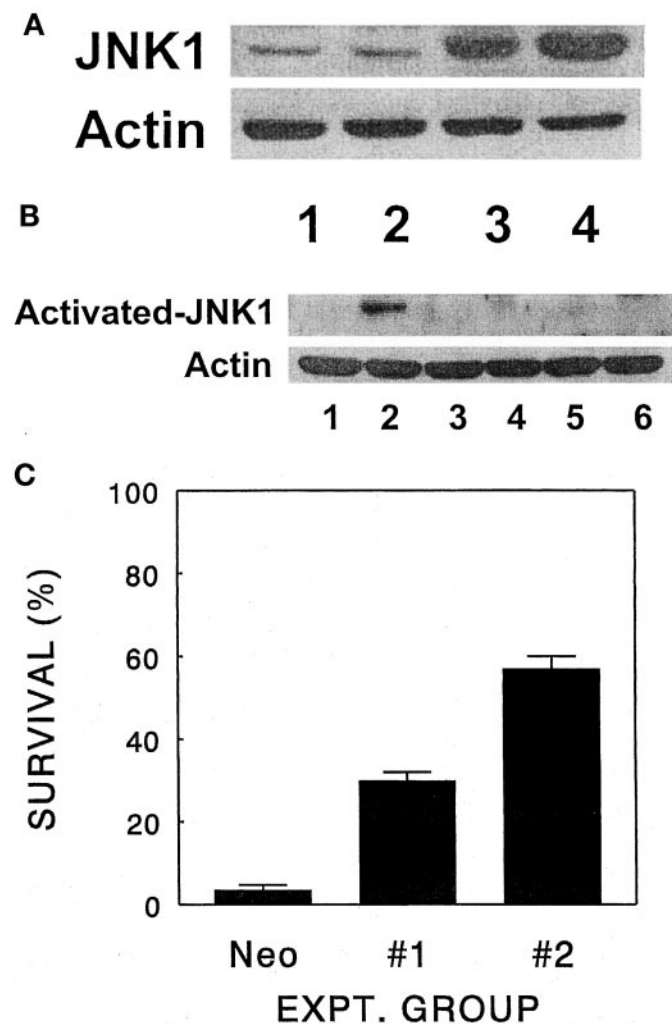


**Fig. 8.** Expression of JNK1 dominant-negative protein and its effect on glucose deprivation plus IV-2-induced JNK activation and cytotoxicity. A, cells were transfected with 2  $\mu\text{g/ml}$  control plasmid (pcDNA3-neo) or 0.5 to 2  $\mu\text{g/ml}$  dominant-negative JNK1 expression plasmid [pcDNA3-FLAG-JNK1(APF)]. After 48 h of incubation, cells were harvested. Cell lysate proteins were separated and immunoblotted by using anti-JNK1 polyclonal antibody. Lane 1, untransfected control cells; lane 2, pcDNA3-neo transfected cells; lane 3, 0.5  $\mu\text{g/ml}$  pcDNA3-FLAG-JNK1(APF)-transfected cells; lane 4, 2  $\mu\text{g/ml}$  pcDNA3-FLAG-JNK1(APF)-transfected cells. Actin was shown as an internal standard. B, cells were transfected with 2  $\mu\text{g/ml}$  pcDNA3-neo (lanes 1 and 2), 0.5  $\mu\text{g/ml}$  pcDNA3-FLAG-JNK1(APF) (lanes 3 and 4), or 2  $\mu\text{g/ml}$  pcDNA3-FLAG-JNK1(APF) (lanes 5 and 6). After 48 h of incubation, cells were harvested (lanes 1, 3, and 5) or exposed to glucose-free medium plus 50  $\mu\text{M}$  IV-2 for 1 h (lanes 2, 4, and 6). Lysates containing equal amounts of protein were separated and immunoblotted by using anti-ACTIVE JNK polyclonal antibody. Actin was used to confirm that an equal amount of protein loaded in each lane. C, cells were transfected with 2  $\mu\text{g/ml}$  pcDNA3-neo (Neo), 0.5  $\mu\text{g/ml}$  pcDNA3-FLAG-JNK1(APF) (#1), or 2  $\mu\text{g/ml}$  pcDNA3-FLAG-JNK1(APF) (#2). After 48 h of incubation, cells were exposed to glucose-free medium plus 50  $\mu\text{M}$  IV-2 for 4 h, and cell survival was determined by the Trypan blue exclusion assay. Error bars represent  $\pm$ S.D. from triplicate experiments.

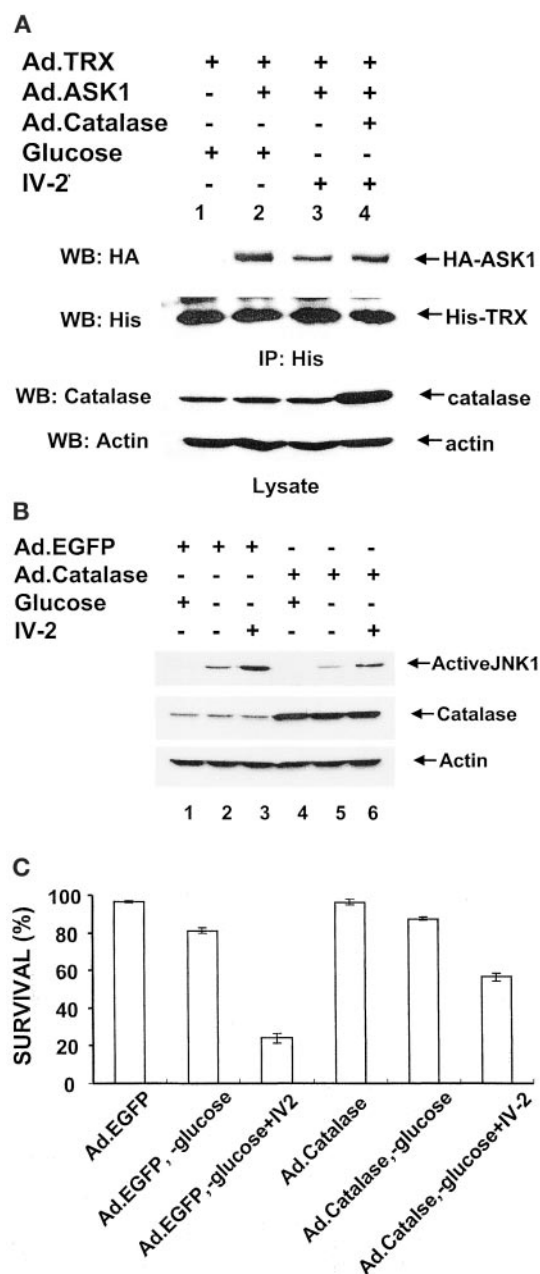


**Fig. 9.** Effect of catalase on glucose deprivation plus IV-2-induced dissociation of TRX from ASK-1, JNK activation, and cytotoxicity. **A**, cells were infected with Ad.TRX at an m.o.i. of 30 pfu/cell, Ad.ASK1 at an m.o.i. of 10 pfu/cell, or adenoviral vectors containing catalase (Ad.Catalase) at an m.o.i. of 100 pfu/cell, respectively. After 24 h of incubation, cells were exposed to complete medium (lane 2) or glucose-free medium in the presence of 50  $\mu$ M IV-2 for 1 h (lanes 3 and 4). Cell lysates were divided into two portions. One portion was immunoprecipitated with anti-His antibody, and then immunoblotted with anti-HA antibody (HA-ASK1) or anti-His antibody (His-TRX). The other portion was immunoblotted with anti-catalase antibody or anti-actin antibody. Actin was used to confirm that similar amounts of proteins were loaded in each lane. **B**, cells were infected with adenoviral vectors containing green fluorescence protein (Ad.EGFP) or Ad.Catalase at an m.o.i. of 100 pfu/cell. After 24 h of incubation, cells were exposed to complete medium (+) or glucose-free medium (-) with (+) or without (-) 50  $\mu$ M IV-2 for 1 h. Cells were harvested, and Western blot analysis was performed as described in Fig. 4 with anti-ACTIVE JNK, anti-catalase, or anti-actin antibodies as the loading control. **C**, cells were infected with adenoviral vectors containing green fluorescence protein (Ad.EGFP) or Ad.Catalase at an m.o.i. of 100 pfu/cell. After 24 h of incubation, cells were exposed to glucose-free medium with or without 50  $\mu$ M IV-2 for 3 h. Cell survival was determined by the Trypan blue exclusion assay. Error bars represent S.D. from triplicate experiments.

intracellular oxidized glutathione. In the absence of substrates necessary for the regeneration of NADPH, glutathione cannot be maintained in the reduced state (Blackburn et al., 1999). It is well known that cells have developed two important defense mechanisms against oxidative stress (Nakamura et al., 1997). One is a thiol reducing buffer consisting of small proteins with redox-active sulfhydryl moieties (e.g., glutathione and thioredoxin). The other is an enzymatic system (e.g., superoxide dismutase, catalase, and glutathione peroxidase). Our results suggest that the combination of glucose deprivation and IV-2 treatment enhances cytotoxicity by decreasing the level of the endogenous thiol buffers. The changes in redox state disrupt the interaction between TRX and ASK1 (Saitoh et al., 1998), subsequently activating the ASK1-SEK1-JNK1 pathway (Ichijo et al., 1997). Overexpression of catalase, an H<sub>2</sub>O<sub>2</sub> scavenger, inhibits glucose deprivation plus IV-2-induced dissociation of TRX from ASK1, JNK1 activation, and cytotoxicity (Fig. 9).

Recent studies reveal that TRX, a redox-regulatory protein, is a negative regulator of ASK1 (Saitoh et al., 1998). TRX binds directly to the N-terminal portion of ASK1 and inhibits ASK1 kinase activity (Saitoh et al., 1998). The interaction between TRX and ASK1 is dependent on the redox status of TRX. TRX contains two redox-active half-cystine residues (Trp-Cys-Gly-Pro-Cys-Lys) in an active center (Holmgren, 1989), which may recognize oxidative stress through catalysis of thiol-disulfide interchange reactions with oxidized molecules. The oxidized TRX, which contains a disulfide bridge in the active site, dissociates from ASK1. The dissociation of TRX and ASK1 results in the activation of ASK1 (Saitoh et al., 1998). ASK1 is a MAPK kinase kinase that can activate both the stress-activated protein kinases (via activation of SEK1) and the p38s (via activation of MKK3 and MKK6) (Ichijo et al., 1997). In this study, we observed that TRX dissociates from ASK1 during glucose deprivation and subsequently activates the ASK1-SEK1-JNK1 signal transduction pathway. IV-2 treatment enhances glucose deprivation-induced JNK1 activation by promoting dissociation of TRX from ASK1.

Several studies have demonstrated that the JNK signal transduction pathway is activated by a variety of cellular stimuli, including mitogenic signals (Minden et al., 1994), oxidative stress (Cui and Douglas, 1997; Qin et al., 1997), DNA-damaging agents (Yu et al., 1996a; Zanke et al., 1996), and chemopreventive drugs (Yu et al., 1996b; Chen et al., 1998). After activation, JNK phosphorylates several transcription factors (Cavigelli et al., 1995; Gupta et al., 1995). It is believed that JNK is involved in both cell-growth and cell-death pathways (Xia et al., 1995; Smith et al., 1997). However, the factors which determine the various outcomes of JNK signaling are still unknown. Chen et al. (1996a,b, 1998) reported that a prolonged activation of JNK was associated with the initiation of cell death. In this study, we demonstrated that IV-2 treatment not only sustained JNK activation, but also promoted JNK activation caused by glucose deprivation in DU-145 cells (Fig. 7). This is probably how IV-2 contributes to metabolic oxidative stress-induced cell death. A fundamental question that remains unanswered is how JNK1 activation leads to cell death. Recent studies have shown that mitochondria are influenced by proapoptotic signal transduction through the JNK pathway (Tournier et al., 2000). JNK is probably involved in Bid cleavage, cyto-

chrome *c* release, or mitochondrial depolarization. These studies suggest that Bid is cleaved by caspase 8 (Li et al., 1998; Luo et al., 1998) or a JNK-mediated caspase-independent mechanism (Tournier et al., 2000). A second potential target of JNK signaling is Bcl-2. Previous studies have shown that the antiapoptotic protein Bcl-2 is phosphorylated by IV-2 treatment (Vogt et al., 2000). Bcl-2 is inactivated by phosphorylation, and its phosphorylation is mediated through activated JNK (Maudrell et al., 1997; Yamamoto et al., 1999). Nonetheless, we shall not rule out any other possibilities. Our data also suggest that not only the disruption of TRX-ASK1 interaction and subsequent stimulation of JNK signaling but also the increase of DNA damage contribute to the hypersensitive phenotype seen with the combined glucose deprivation and IV-2 treatment (Figs. 1 and 2). These genotoxic events are probably inhibited by scavenging H<sub>2</sub>O<sub>2</sub> in the catalase-overexpressing cells (Fig. 9C). This possibility needs to be further investigated. Although we believe that many critical questions still remain to be answered to understand the mechanisms of IV-2-augmented glucose deprivation-induced cytotoxicity, our proposed model provides important information for understanding how signal transduction pathways or genotoxic events are involved in metabolic oxidative stress-induced cell death.

## References

- Aslund F and Beckwith J (1999) Bridge over troubled waters: sensing stress by disulfide bond formation. *Cell* **96**:751–753.
- Blackburn RV, Spitz DR, Liu X, Galoforo SS, Sim JE, Ridnour LA, Chen JC, Davis BH, Corry PM, and Lee YJ (1999) Metabolic oxidative stress activates signal transduction and gene expression during glucose deprivation in human tumor cells. *Free Rad Biol Med* **26**:419–430.
- Cavigelli M, Dolfi F, Claret FX, and Karin M (1995) Induction of *c-fos* expression through JNK-mediated TCF/Elk-1 phosphorylation. *EMBO (Eur Mol Biol Organ) J* **14**:5957–5964.
- Chen Y-R, Meyer CF, and Tan T-H (1996a) Persistent activation of c-Jun N-terminal kinase 1 (JNK1) in gamma radiation-induced apoptosis. *J Biol Chem* **271**:631–634.
- Chen Y-R, Wang W, Kong AN, and Tan TH (1998) Molecular mechanisms of c-Jun N-terminal kinase-mediated apoptosis induced by anticarcinogenic isothiocyanates. *J Biol Chem* **273**:1769–1775.
- Chen Y-R, Wang X, Templeton D, Davis RJ, and Tan T-H (1996b) The role of c-Jun N-terminal kinase (JNK) in apoptosis induced by ultraviolet C and  $\gamma$  radiation: duration of JNK activation may determine cell death and proliferation. *J Biol Chem* **271**:31929–31936.
- Cui X-L and Douglas JG (1997) Arachidonic acid activates c-jun N-terminal kinase through NADPH oxidase in rabbit proximal tubular epithelial cells. *Proc Natl Acad Sci USA* **94**:3771–3776.
- Gupta S, Campbell D, Derijard B, and Davis RJ (1995) Transcription factor ATF2 regulation by the JNK signal transduction pathway. *Science (Wash DC)* **267**:389–393.
- Hardy S, Kitamura M, Harris-Stansil T, Dai Y, and Phipps ML (1997) Construction of adenovirus vectors through Cre-*lox* recombination. *J Virol* **71**:1842–1849.
- Hirota K, Matsui M, Murata M, Takashima Y, Cheng FS, Itoh T, Fukuda K, and Yodoi J (2000) Nucleoredoxin, glutaredoxin, and thioredoxin differentially regulate NF- $\kappa$ B, AP-1 and CREB activation in HEK293 cells. *Biochem Biophys Res Commun* **274**:177–182.
- Holmgren A (1985) Thioredoxin. *Annu Rev Biochem* **54**:237–271.
- Holmgren A (1989) Thioredoxin and glutaredoxin systems. *J Biol Chem* **264**:13963–13966.
- Ichijo H, Nishida E, Irie K, ten Dijke P, Saitoh M, Moriguchi T, Takagi M, Matsmoto K, Miyazono K, and Gotoh Y (1997) Induction of apoptosis by ASK1, a mammalian MAPKKK that activates SAPK/JNK and p38 signaling pathways. *Science (Wash DC)* **275**:90–94.
- Iwata S, Hori T, Sato N, Hirota K, Sasada T, Mitsui A, Hirakawa T, and Yodoi J (1997) Adult T cell leukemia (ATL)-derived factor/human thioredoxin prevents apoptosis of lymphoid cells induced by L-cystine and glutathione depletion: possible involvement of thiol-mediated redox regulation in apoptosis caused by pro-oxidant state. *J Immunol* **158**:3108–3117.
- Kirkpatrick DL, Kuperus M, Dowdeswell M, Potier N, Donald LJ, Kunkel M, Berggren M, Angulo M, and Powis G (1998) Mechanisms of inhibition of the thioredoxin growth factor system by antitumor 2-imidazolyl disulfides. *Biochem Pharmacol* **55**:987–994.
- Laemmli UK (1970) Cleavage of structural proteins during the assembly of the head of bacteriophage T4. *Nature (Lond)* **227**:680–685.
- Lan J, Henshall DC, Simon RP, and Chen J (2000) Formation of the base modification 8-hydroxyl-2'-deoxyguanosine and DNA fragmentation following seizures induced by systemic kainic acid in the rat. *J Neurochem* **74**:302–309.
- Lee YJ, Galoforo SS, Berns CM, Chen JC, Davis BH, Sim JE, Corry PM, and Spitz DR (1998) Glucose deprivation-induced cytotoxicity and alterations in mitogen-activated protein kinase activation are mediated by oxidative stress in multidrug-resistant human breast carcinoma cells. *J Biol Chem* **273**:5294–5299.
- Lee YJ, Galoforo SS, Sim JE, Ridnour LA, Choi J, Forman HJ, Corry PM, and Spitz DR (2000) Dominant-negative Jun N-terminal protein kinase (JNK-1) inhibits metabolic oxidative stress during glucose deprivation in a human breast carcinoma cell line. *Free Radic Biol Med* **28**:575–584.
- Li H, Zhu H, Xu CJ, and Yuan J (1998) Cleavage of BID by caspase 8 mediates the mitochondrial damage in the Fas pathway of apoptosis. *Cell* **94**:491–501.
- Luo X, Budihardjo I, Zou H, Slaughter C, and Wang X (1998) Bid, a Bcl2 interacting protein, mediates cytochrome *c* release from mitochondria in response to activation of cell surface death receptors. *Cell* **94**:481–490.
- Matthews JR, Wakasugi N, Virelizier J-L, Yodoi J, and Hay RT (1992) Thioredoxin regulates the DNA binding activity of NF- $\kappa$ B by reduction of a disulfide bond involving cysteine 62. *Nucleic Acids Res* **20**:3821–3830.
- Maudrell K, Antonsson B, Magnenat E, Camps M, Muda M, Chabert C, Gillieron C, Boschert U, Vial-Knecht E, Martinou J-C, et al. (1997) Bcl-2 undergoes phosphorylation by c-Jun N-terminal kinase/stress-activated protein kinases in the presence of the constitutively active GTP-binding protein Rac1. *J Biol Chem* **272**:25238–25242.
- Minden A, Lin A, Smeal T, Derijard B, Cobb M, Davis R, and Karin M (1994) c-Jun N-terminal phosphorylation correlates with activation of the JNK subgroup but not the ERK subgroup of mitogen-activated protein kinases. *Mol Cell Biol* **14**:6683–6688.
- Nagayama T, Simon RP, Chen D, Henshall DC, Pei W, Stetler RA, and Chen J (2000) Activation of poly(ADP-ribose) polymerase in the rat hippocampus may contribute to cellular recovery following sublethal transient global ischemia. *J Neurochem* **74**:1636–1645.
- Nakamura H, Nakamura K, and Yodoi J (1997) Redox regulation of cellular activation. *Annu Rev Immunol* **15**:351–369.
- Qin S, Minami Y, Hibi M, Kurosaki T, and Yamamura H (1997) Syk-dependent and -independent signaling cascades in B cells elicited by osmotic and oxidative stress. *J Biol Chem* **272**:2098–2103.
- Saitoh M, Nishitoh H, Fujii M, Takeda K, Tobiume K, Sawada Y, Kawabata M, Miyazono K, and Ichijo H (1998) Mammalian thioredoxin is direct inhibitor of apoptosis signal-regulating kinase (ASK) 1. *EMBO (Eur Mol Biol Organ) J* **17**:2596–2606.
- Smith A, Ramos-Morales F, Ashworth A, and Collins M (1997) A role for JNK/SAPK in proliferation, but not apoptosis, of IL-3-dependent cells. *Curr Biol* **7**:893–896.
- Spector A, Yan G-Z, Huang R-RC, McDermott MJ, Gascoyne PRC, and Pigiet V (1988) The effect of H<sub>2</sub>O<sub>2</sub> upon thioredoxin-enriched lens epithelial cells. *J Biol Chem* **263**:4984–4990.
- Takemoto T, Zhang Q-M, and Yonei S (1998) Different mechanisms of thioredoxin in its reduced and oxidized forms in defense against hydrogen peroxide in *Escherichia coli*. *Free Radic Biol Med* **24**:556–562.
- Tournier C, Hess P, Yang DD, Xu J, Turner TK, Nimnual A, Bar-Sagi D, Jones SN, Flavell RA, and Davis RJ (2000) Requirement of JNK for stress-induced activation of the cytochrome *c*-mediated death pathway. *Science (Wash DC)* **288**:870–874.
- Vogt A, Tamura K, Watson S, and Lazo JS (2000) Antitumor imidazolyl disulfide IV-2 causes irreversible G<sub>2</sub>M cell cycle arrest without hyperphosphorylation of cyclin-dependent kinase Cdk1. *J Pharmacol Exp Ther* **294**:1070–1075.
- Wakasugi N, Tagaya Y, Wakasugi A, Mitsui M, Maeda M, Yodoi J, and Tursz T (1990) Adult T-cell leukemia-derived factor/thioredoxin produced by both human T-lymphotropic virus type 1 and Epstein-Barr virus-transformed lymphocytes, acts as an autocrine growth factor and synergized with interleukin-1 and interleukin-2. *Proc Natl Acad Sci USA* **87**:8282–8286.
- Xia Z, Dickens M, Raingeaud J, Davis RJ, and Greenberg ME (1995) Opposing effects of ERK and JNK-p38 MAP kinases on apoptosis. *Science (Wash DC)* **270**:1326–1331.
- Yamamoto K, Ichijo H, and Korsmeyer SJ (1999) BCL-2 is phosphorylated and inactivated by an ASK1/Jun N-terminal protein kinase pathway normally activated at G<sub>2</sub>M. *Mol Cell Biol* **19**:8469–8478.
- Yu R, Jiao J-J, Tan T-H, and Kong A-NT (1996a) Phenethyl isothiocyanate, a natural chemopreventive agent, activates c-Jun N-terminal kinase 1. *Cancer Res* **56**:2954–2959.
- Yu R, Shtil AA, Tan T-H, Roninson IB, and Kong A-NT (1996b) Adriamycin activates c-jun N-terminal kinase in human leukemia cells: a relevance to apoptosis. *Cancer Lett* **107**:73–81.
- Yuasa T, Ohno S, Kehrl JH, and Kyriakis JM (1998) Tumor necrosis factor signaling to stress-activated protein kinase (SAPK)/Jun NH2-terminal kinase (JNK) and p38. Germinal center kinase couples TRAF2 to mitogen-activated protein kinase/ERK kinase 1 and SAPK while receptor interacting protein associates with a mitogen-activated protein kinase kinase upstream of MKK6 and p38. *J Biol Chem* **273**:22681–22692.
- Zanke BW, Boudreau K, Rubie E, Winnett E, Tibbles LA, Zon L, Kyriakis J, Liu F-F, and Woodgett JR (1996) The stress-activated protein kinase pathway mediates cell death after injury induced by *cis*-platinum, UV irradiation or heat. *Curr Biol* **6**:606–613.

**Address correspondence to:** Dr. Yong J. Lee, Department of Surgery, University of Pittsburgh Cancer Institute, E1056 BST, 200 Lothrop Street, Pittsburgh, PA 15213. E-mail: leeyj@msx.upmc.edu